Deposition of Palladium Overlayers on Oxygen-Precovered Ruthenium(100)

Stephen Poulston,* Mintcho Tikhov, and Richard M. Lambert

Department of Chemistry, University of Cambridge, Lensfield Road, Cambridge, U.K.

Received: August 22, 1996; In Final Form: November 4, 1996[⊗]

We have studied the deposition of Pd on oxygen-precovered Ru(100) at 300 K as a function of both oxygen and Pd coverage. A layered growth of Pd similar to that observed on clean Ru is maintained in the presence of preadsorbed oxygen. This results in complete removal of oxygen from contact with the Ru surface with efficient diffusion to the Pd−vacuum interface. This was confirmed with the complete reactive removal of preadsorbed oxygen by CO at 300 K for $\theta_{Pd} > 6$ ML. The out-diffused oxygen overlayer is unusually dense and cannot be made by dissociative chemisorption of O_2 on Pd overlayers on Ru(100). This additional oxygen is desorbed from a new thermal desorption state at 700 K with the remaining oxygen desorbing at 1037 K for $\theta_{Pd} > 2$ ML.

Introduction

Studies of metal−metal systems usually involve rigorously cleaned substrates in UHV. However it is known that the presence of molecularly adsorbed gases such as CO or H_2O and dissociatively adsorbed O, N, C, H, and S can influence the growth process of metals on metals.[1−11] In some cases these impurities are known to enhance layer-by-layer growth.[1] Conversely oxygen adsorption on a Ru(001) surface causes Au and Ag to grow in a more three-dimensional manner.[7−9] The adsorbed molecule/atom can remain in contact with the substrate as for Au deposition on oxygen-precovered Ru(001), "float" off the admetal−substrate interface to the admetal−vacuum interface,[5,11] or react with the oxygen to form an oxide-like overlayer.[10] The behavior of a particular system would be expected to depend upon factors such as the relative strength of the interaction between the nonmetal adsorbate and the substrate/admetal and the mobility over the surface of the two adsorbates. The reasons for the variation in metal−metal growth mode with chemical modification of the substrate may lie in the adsorbate-induced changes in the surface and interface free energies and strain, factors which influence the growth process.[12] A UHV study of metal deposition on an oxygen-precovered surface is therefore useful in understanding both the interaction of the evaporated metal with coadsorbed oxygen and the parameters that determine the growth modes of the metal films.

Here we report on the deposition of Pd on oxygen-precovered Ru(100). The deposition of Pd on transition metal substrates has been extensively studied,[13] and we have previously reported on the growth mode and thermal stability of Pd overlayers on Ru(100) using low-energy electron diffraction (LEED), Auger electron spectroscopy (AES), and temperature-programmed desorption (TPD) measurements.[14] These results are consistent with a layer-by-layer type growth of Pd at 300 K to coverages of at least 4 ML (1 ML $= 8.6 \times 10^{14}$ atoms cm^{-2}). LEED indicated a pseudomorphic (1×1) pattern for coverages of ∼2−6 ML, coverages <2 ML yielding $1\times n$ ($n = 2, 3$) patterns. Pd films in excess of 2 ML were unstable toward agglomeration on annealing at temperatures > 500 K. Pd thermal desorption profiles show a single desorption peak (α'_1) at ∼1360−1380 K for coverages up to 2 ML. For >2 ML Pd a second desorption state (α'_2) appears at lower temperature, shifting to higher temperature with increasing coverage, which is due to multilayer desorption from increasingly large three-dimensional agglomerates. Additionally we have previously studied the adsorption of oxygen on Ru(100)[15] and on Pd-precovered Ru(100).[16]

Experimental Section

Experiments were performed in an ultrahigh-vacuum chamber operated at a base pressure of $\sim 1 \times 10^{-10}$ Torr. It was equipped with a retarding field analyzer, glancing incidence electron gun for Auger measurements, quadrupole mass spectrometer, ion gun, capillary array gas doser, and Pd deposition source consisting of a W filament wrapped with Pd wire. The Ru(100) substrate was cleaned using a well-established procedure[17] involving cycles of argon bombardment, annealing, and oxygen adsorption/desorption. Gas exposures are quoted in langmuirs (L) where 1 L $= 1 \times 10^{-6}$ Torr s. Pd coverages are quoted in monolayers (ML), where 1 ML $= 8.6 \times 10^{14}$ atoms cm^{-2}, and were calibrated using a combination of LEED, TPD, and AES as described in ref 14.

Adsorption sequences on Ru(100) are represented by abbreviations of the type $Pd_x/O_1/Ru(100)$, which indicates Pd deposition on oxygen-precovered Ru(100) where the suffix x and 1 represent the Pd and oxygen coverages in monolayers. The saturation oxygen coverage on Ru(100) following a 20 L oxygen exposure is 1 ML.[15]

Results and Discussion

The uptake of Pd on clean and oxygen-presaturated Ru(100) are compared in Figure 1, which shows the variation in Pd, Ru, and O Auger intensities as a function of Pd deposition time. Pd deposition on the clean surface (filled symbols) results in a layer-by-layer growth mode with the first close packed layer of 2 ML Pd being completed after 8 min deposition time. Completion of this layer is accompanied by a change in the slope of the Pd(328 eV) and Ru(274 eV) Auger intensity signals. The uptake of Pd on oxygen-presaturated Ru(100) (open symbols) closely resembled that observed on clean Ru, indicating essentially layered growth of the Pd even in the presence of preadsorbed oxygen. The most significant difference between the two cases being that for equivalent Pd doses > 1 ML, the Pd intensity was somewhat lower in the case of the oxygenated surface. Note, however, that although the Ru(274 eV) signal was completely attenuated by 8 ML of Pd, *there was only a*

* Corresponding author address: Department of Chemistry, University of Reading, Whiteknights Park, Reading, RG6 6AD, U.K. Email: scspouls@reading.ac.uk. FAX: 44-(0)1734-316331.

[⊗] Abstract published in *Advance ACS Abstracts,* December 15, 1996.

S1089-5647(96)02604-1 CCC: $14.00

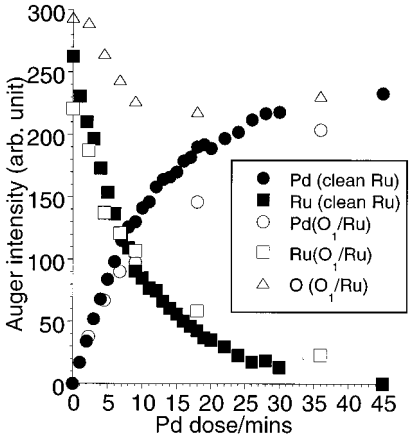

Figure 1. Pd(328 eV), Ru(274 eV), and O(520 eV) Auger intensities as a function of Pd deposition time on clean and oxygen-presaturated (20 L) Ru(100).

small decrease in the O(520 eV)intensity at this point. Furthermore, additional Pd deposition up to 20 ML also led to no further decrease of the O(520 eV) intensity. As will be confirmed subsequently, this behavior represents the removal of oxygen from contact with the Ru and transport to the Pd−vacuum interface. The initial reduction of the oxygen signal may be due to a broadening of the oxygen Auger peak shape, resulting in a decrease in the peak-to-peak intensity of the signal. The lower Pd intensity for equivalent doses in the case of the oxygenated surface can therefore be partly explained by additional attenuation from the oxygen overlayer. This only becomes significant for $\theta_{Pd} > 1$ ML, as up to this point the oxygen and Pd adatoms can exist as a single close packed layer both in contact with the Ru surface.

Oxygen desorption profiles for varying amounts of Pd deposited on oxygen-presaturated Ru are shown in Figure 2a. Increasing the Pd coverage led to a decrease in the amount of oxygen desorbed from states associated with clean Ru and to development of a new desorption state, α_1, at ∼1037 K. The β_2 Ru−O_2 state (at ∼1400 K) was completely quenched by addition of ∼1 ML Pd, while the β_1 Ru−O_2 state (at ∼1200 K) persisted until completion of the second Pd monolayer; at this point only the sharp α_1 peak remained. For thicker (>8 ML) Pd overlayers another new oxygen desorption feature, α_2, appears at 700 K. The growth of the α_2 state was accompanied by a decrease in the desorption yield from the α_1 state. For subsaturation oxygen precoverages, addition of 2−8 ML Pd again led to all the oxygen being desorbed from the α_1 state at ∼1037 K. Higher (>8 ML) Pd coverages resulted additionally in appearance of the α_2 state, *provided that the Ru oxygen precoverage exceeded ∼75% of the saturation value*. For oxygen precoverages lower than this threshold value no α_2 desorption appeared, whatever the subsequent Pd loading. It is important to note that the α_2 peak found for the $Pd_{>8}/O_1/Ru$ system is not observed for the reverse sequence of adsorption $O/Pd_x/Ru(100)$. Equivalent oxygen desorption spectra for this adsorption sequence are shown in Figure 2b. This difference suggests an explanation for the α_2 peak in the ability of the Ru(100) to adsorb ∼20% more oxygen than a thick (>8 ML) Pd overlayer. The extra oxygen when transported to the Pd surface is therefore accommodated in a new state, α_2. This conclusion was supported by AES data, which confirm that ∼20% less oxygen was adsorbed on a 8 ML Pd overlayer than on clean Ru(100). The precise explanation is however complicated by agglomeration of the Pd overlayer during the TPD experiment; this is discussed in more detail below.

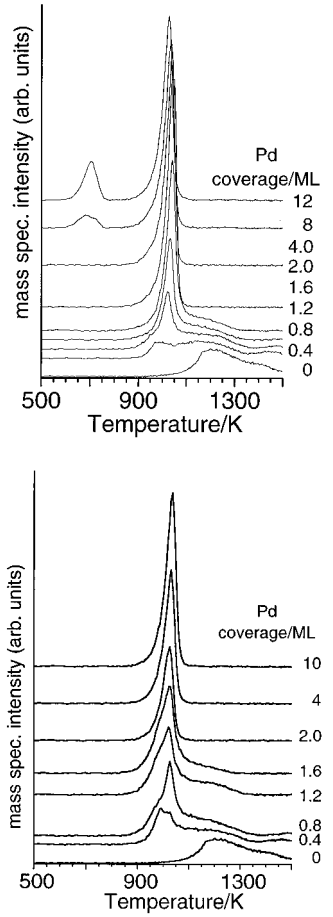

Figure 2. (a, top) Oxygen thermal desorption profiles for the $Pd_x/O_1/Ru$ system. The profiles at different Pd coverages, for this and part b, are offset for clarity, and the Pd coverage associated with each profile is indicated on the right of the figure, the top profile corresponding to the highest Pd coverage and the Pd coverage decreasing for lower profiles as indicated. (b, bottom) Oxygen thermal desorption profiles for 20 L oxygen exposure on the $O/Pd_x/Ru$ system.

The driving force for the "float out" of oxygen does not seem to lie in improved oxygen−metal bond energy, as the O−Ru bond strength is higher than O−Pd. The driving force would therefore seem to lie in the stability of the Pd−Ru interface being greater than that of Ru−O−Pd. Similar float out behavior has been reported for other systems including deposition of Cu on oxygen-presaturated Ru(001), which results in all but ∼15% of the oxygen being removed from the Ru interface,[5] and deposition of Pd on CO-precovered W(110).[6]

The oxygen α_1 desorption feature is invariant in peak shape and desorption temperature for both sequences of adsorption and different Pd and oxygen coverages. This suggests that in all cases there is a common rate-determining step for the recombinative desorption. The mobility of the oxygen at 1000 K would probably be high, and so the desorption process is unlikely to be diffusion rate limited. A more likely candidate is the actual recombination step. By the desorption temperature the $Pd_{>2}/O_1/Ru(100)$ overlayer has already undergone extensive agglomeration (see AES and LEED results below), leaving a 2 ML thick continuous layer of Pd surmounted by small highly three-dimensional islands. The 2 ML thick layer therefore dominates the available surface, presenting an essentially common surface, by 1000 K, for a wide range of starting conditions. This could lead to the common α_1 desorption state. For the α_2 desorption peak at 700 K the agglomeration may not however be sufficiently complete for the surface to be invariant with Pd coverage, some change in the overlayer

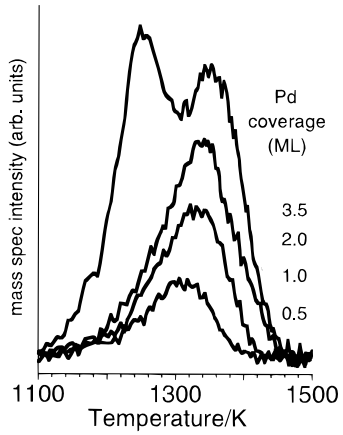

Figure 3. Pd desorption profiles for the $Pd_x/O_1/Ru$ system.

occurring at ~8 ML. In this respect it is worth noting that for deposition of Pd on clean Ru(100) a change in the surface structure occurs at around this coverage.[14]

On oxygenated Ru, the Pd desorption spectra for Pd coverages > 2 ML were the same as for the corresponding Pd coverage on clean Ru,[14] the α'_1 state occurring at 1370 ± 10 K. However, for lower Pd coverages (<2 ML), where oxygen is still present on the surface *during* Pd desorption, the α'_1 desorption is shifted to lower temperature relative to the oxygen-free system. In the case of a 0.5 ML Pd coverage the downward shift is 50 K; this is illustrated in Figure 3. For 0.5 ML Pd the downward shift corresponds to a decrease in the Pd desorption energy of ~16 kJ/mol when E_d is determined from the single spectra formula of Redhead.[19] This shift decreased with increasing Pd coverage and *decreasing* oxygen precoverage. The presence of oxygen in contact with Ru is therefore responsible for the desorption temperature shift of the Pd, possibly due to an electronic interaction between the Ru and oxygen, leading to a weakening of the Pd−Ru bond strength. No indication of palladium oxide desorption was observed using TPD. This is not surprising considering the conditions required for oxidation of bulk Pd (prolonged heating to ~900 K in oxygen at several Torr pressure), which are far more vigorous than those used here.[20]

The thermal desorption results were consistent with the temperature dependence of the O(520 eV), Pd(328 eV), and Ru(274 eV) Auger intensities (Figure 4). Figure 4a shows the variation in the O(520 eV) Auger signal. It indicates the onset of oxygen desorption (i.e. lowering of the O(520 eV) Auger intensity) at lower temperature in the presence of Pd. For Pd coverages > 2 ML oxygen desorption from the α_1 state is complete by 1000 K. In the case of a 10 ML Pd film the oxygen signal shows a knee at ~700 K, reflecting completion of desorption from the α_2 state. For Pd coverages > 2 ML the Pd(328 eV) intensity showed a sharp drop on annealing to ~500 K (Figure 4b): this change is larger than that observed in the absence of oxygen, indicating oxygen-assisted agglomeration of the Pd film, which was confirmed by a corresponding increase in the Ru(274 eV) signal, Figure 4c. The Pd and Ru Auger intensities on annealing to 750−800 K are compatible with formation of a Pd layer of ~2 ML thickness. With the onset of oxygen desorption at ~900 K, the Pd signal then *increased* to a value characteristic of the oxygen-free overlayer, leveling off before the onset of Pd desorption at ~1100 K; this increase was accompanied by a corresponding decrease in the Ru(274 eV) signal. That is, oxygen removal leads to a slight rewetting of Ru by Pd. The additional agglomeration above that observed for Pd_x/Ru could be explained by more three-dimensional islands on top of a 2 ML thick Pd film. This conclusion is supported

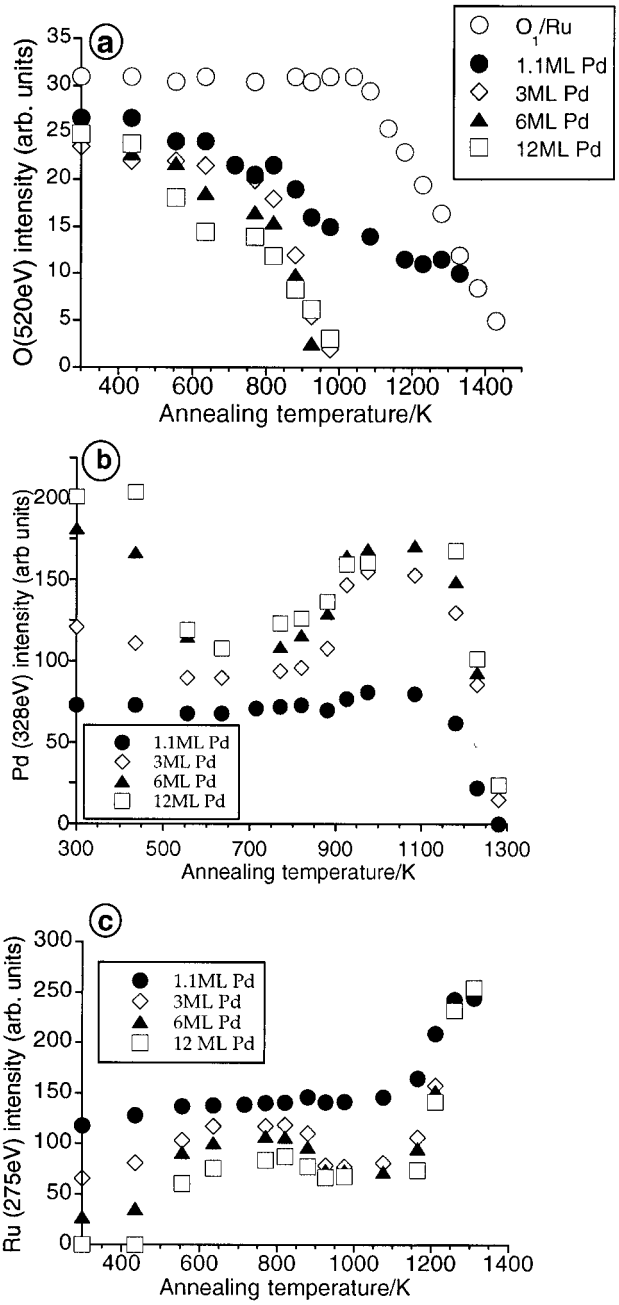

Figure 4. Variation of the Auger signal intensities for the $Pd_x/O_1/Ru$ system on annealing: (a) O(520 eV), (b) Pd(328 eV), (c) Ru(274 eV).

by LEED, which shows a pattern characteristic of the $O/Pd_2/Ru(100)$ system *with no additional structure from the Pd islands* at 900 K, unlike the equivalent Pd_x/Ru system (see below). More three-dimensional Pd islands would be favored by a lower surface free energy of the 2 ML Pd film in the presence of adsorbed oxygen

Coadsorbate-induced compression effects of overlayers on single-crystal surfaces have been observed for several systems.[15,20−22] In particular the addition of Cu[22] and Au[23] to O_2-precovered Ru(001) leads to an increase in the local oxygen coverage. To examine this possibility in the present case, Pd was deposited on the Ru surface precovered with a *subsaturation* amount of oxygen so as to form a good c(2×4) pattern. It is important to note that dissociative oxygen adsorption on Ru(100) at 300 K leads to a series of LEED patterns commencing with c(2×4) and progressing via a "split (2×1)" to a (2×1)-p2mg pattern corresponding to a saturation 1 ML coverage. No change in the initial *c*(2×4) pattern (Figure 5A) was observed

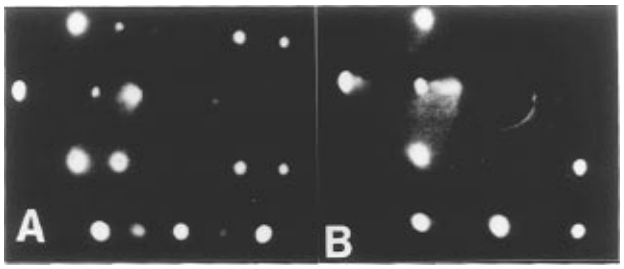

Figure 5. LEED patterns for addition of Pd to oxygen-precovered Ru(100): (A) c(2×4) $O_{0.5}$/Ru, 82 eV; (B) *c*(2×4) $O_{0.5}$/Ru + 1.2 ML Pd, 82 eV, giving a (2×1)-*p2mg* pattern.

on addition of 0.5 ML Pd, but with further Pd there was a progressive change to the (2×1)-p2mg phase (Figure 5B) via the "split (2×1)", the LEED pattern sequence being very similar to that observed for increasing oxygen exposure on clean Ru(100).[15] Appearance of characteristic O/Ru(100) patterns suggests formation of separate islands of oxygen and Pd. At 300 K addition of >1.5 ML Pd to oxygen *presaturated* Ru(100) led to a fading of the pattern, leaving a diffuse (1×1) pattern after addition of ∼2 ML.

The thermal behavior of Pd_x/O_1/Ru(100) systems was also observed with LEED. For overlayers of composition $Pd_{>2}/O_1$/Ru, annealing led to the observation of features attributable to oxygen and Pd components of the overlayer. Annealing to 890 K led to the gradual appearance of a sharp (2×1)-p2mg pattern, which may be assigned to an ordered oxygen overlayer on a pseudomorphic Pd overlayer of ∼2 ML thickness (890 K corresponds to maximum agglomeration in the Pd overlayer). Indeed the same LEED pattern was observed with oxygen adsorption on Pd_2/Ru(100). With further annealing to 990 K (oxygen desorption from the α_1 state) the LEED pattern reverted to (1×1). Annealing also resulted in the simultaneous formation of a (1×*n*) pattern, which consisted of distinct spots at ∼600 K. The (1×*n*) pattern was removed completely on further annealing to 900 K, leaving only a (2×1)-p2mg pattern very similar to that shown in Figure 5B. The (1×*n*) feature was likely to have resulted from Pd islands in the overlayer. This would explain their disappearance at 900 K, by which point, due to the extent of the Pd agglomeration, Pd islands on top of the 2 ML pseudomorphic Pd layer were no longer large enough to be observed in LEED. Their observation in the form of a distinct (1×*n*) pattern at 600 K, though not at 300 K, could be attributed to increased ordering of the Pd with this mild annealing. At temperatures > 1000 K the LEED behavior followed that for the equivalent oxygen-free Pd/Ru system.[14] With respreading of the Pd overlayer at ∼1100 K signs of faceting were observed in the Pd/Ru system in the form of energy dependent diffraction features along the [001] Ru direction. The clean surface (1×1) pattern of Ru(100) was recovered by annealing to 1300 K.

For Pd coverages < 2 ML annealing to 900 K again resulted in formation of a (2×1)-p2mg pattern, though this persisted to higher annealing temperatures than for θ_{Pd} > 2 ML. The persistence of an O related pattern above 1100 K can be attributed to occupancy of β_1 and β_2 Ru−O states, which desorbed at higher temperature than the α_1 Pd−O state. On annealing to temperatures sufficient to desorb Pd, but at which some oxygen remained, the appropriate O_x/Ru(100) LEED pattern (split (2×1), c(2×4)) could be distinguished.

Pd surfaces are extremely efficient at promoting CO_2 formation from coadsorbed CO and O_2 in UHV;[24] however, Ru is completely inactive toward CO oxidation in UHV at 300 K.[15] In light of this, CO titration experiments were performed on the Pd_x/O_1/Ru system to further confirm the presence of oxygen

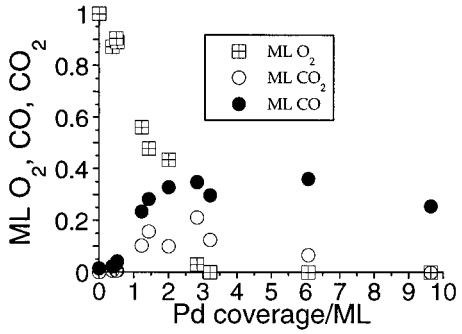

Figure 6. CO, O_2, and CO_2 thermal desorption yields as a function of Pd coverage for TPD taken after Pd_x/O_1/Ru systems were titrated with a 50 L CO exposure.

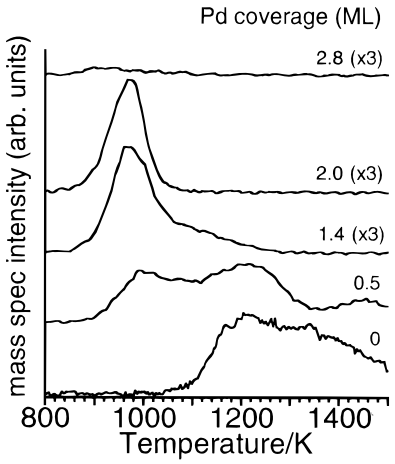

Figure 7. O_2 thermal desorption profiles taken following CO titration of Pd_x/O_1/Ru.

close to or on top of the Pd overlayer. Figure 6 shows the integrated thermal desorption yields for O_2, CO, and CO_2 when a Pd_x/O_1/Ru surface was titrated with a 50 L CO exposure. As was the case with CO on O/Pd_x/Ru,[15] the O_2 desorption yield decreased with increasing Pd coverage, reaching zero at ∼3 ML; this was accompanied by an increase in the CO desorption yield. The latter is due to reactive removal of oxygen by CO to form CO_2, which immediately desorbs, freeing the surface for repopulation by CO adsorbed from the gas phase. Oxygen desorption profiles (Figure 7) closely resembled those obtained in the Pd_x/O_1/Ru system although with a reduction in the intensity of the component attributed to oxygen desorption from Pd sites. Note that at 2 ML Pd there was still oxygen desorption although entirely from the α_1 state, indicating oxygen desorption from Pd, this oxygen being unreactive toward CO oxidation at 300 K. For Pd coverages from 6 up to at least 20 ML only CO desorption was observed. This confirmed that even at 300 K all the preadsorbed oxygen must be at the surface and so available for reaction with CO. It is interesting to note that it was not until a Pd coverage of ∼6 ML was reached that the Pd adopted the CO oxidation properties of bulk Pd and all the oxygen was consumed at 300 K. This behavior is very similar to that produced for oxygen adsorbed on Pd-precovered Ru(100) and can be accounted for by the gradual adoption of bulklike Pd electronic properties with increasing coverage to ∼6 ML.[16]

Conclusions

1. Deposition of Pd on oxygen presaturated Ru leads to removal of the oxygen from contact with the Ru to the Pd−vacuum interface. There is therefore a similarity in the behavior of this system with that of the reverse sequence of adsorption,

$O/Pd_x/Ru(100)$. However, one noticeable difference between the two systems was the observation of a second new oxygen desorption feature in $Pd_x/O_{1.0}/Ru$ systems but not those of $O/Pd_x/Ru$ when the Pd coverage was in excess of 8 ML. This feature is a result of the higher saturation oxygen coverage of clean Ru(100) when compared with a thick Pd overlayer.

2. LEED observations indicate that the addition of Pd to oxygen-precovered surfaces leads initially to the formation of separate islands of Pd and oxygen on the surface and can increase the local oxygen density.

3. Agglomeration of the Pd overlayer occurs with annealing > 500 K. By 900 K a well-ordered oxygen overlayer was formed on a 2 ML thick Pd film with the excess Pd accommodated in highly three-dimensional islands. Oxygen desorption led to some rewetting of the surface by Pd from these islands.

4. The CO oxidation capability of the preadsorbed oxygen in $Pd_x/O_1/Ru(100)$ systems is very similar to that for postadsorbed oxygen on Pd overlayers, confirming the removal of oxygen from contact with the Ru to the Pd−vacuum interface in the former case. In particular it should be noted that for θ_{Pd} > 8 ML CO is the only desorption product, indicating that all the oxygen can be reactively removed at 300 K and therefore must be present at the surface.

References and Notes

(1) Egelhoff, W. F.; Steigerwald, D. A. *J. Vac. Sci. Technol.* **1989**, *A7*, 2167.
(2) Gaigher, H. L.; Berg, N. G.; Malherbe, J. B. *Thin Solid Films* **1986**, *137*, 337.
(3) Pavlovska, A.; Bauer, E. *Surf. Sci.* **1986**, *175*, 369.
(4) Houston, J. E.; O'Neill, D. G.; Gomer, R. *Surf. Sci.* **1991**, *244*, 221.
(5) Kalki, K.; Schick, M.; Ceballos, G.; Wandelt, K. *Thin Solid Films* **1993**, *228*, 36.
(6) Lin, J. C.; Shamir, N.; Gomer, R. *Surf. Sci.* **1990**, *226*, 26.
(7) Bludau, B.; Skottke, M.; Pennemann, B.; Mrozek, P.; Wandelt., K. *Vacuum* **1990**, *41*, 1106.
(8) Schroder, J.; Gunther, C.; Hwang, R. Q.; Behm, R. J. *Ultramicroscopy* **1992**, *42*−*44*, 475.
(9) Malic, I.; Hrbek, J.; *J. Vac. Sci. Technol.* **1991**, *A9*, 1806.
(10) Poulston, S.; Tikhov, M.; Lambert, R. M. *Surf. Sci.* **1993**, *287/288*, 969.
(11) Stanners, C. D.; Cremer, P. S.; Wilk, D. E.; Shen, Y. R.; Somorjai, G. A. *Surf. Sci.* **1995**, *334*, 95.
(12) Bauer, E. *Appl. Surf. Sci.* **1982**, *11*, 479.
(13) Rodriguez, J. A.; Goodman, D. W. *J. Phys. Chem.* **1991**, *95*, 4196.
(14) Poulston, S.; Tikhov, M.; Lambert, R. M. *Surf. Sci*. **1996**, *352*−*354*, 41.
(15) Poulston, S.; Tikhov, M.; Lambert, R. M. *Surf. Rev. Lett.* **1994**, *1*, 655.
(16) Poulston, S.; Tikhov, M.; Lambert, R. M. *Catal. Lett.*, in press.
(17) Musket, R. G.; McClean, W.; Colmenares, C. A.; Makowiecki, D. M.; Siekhaus, W. J. *Appl. Surf. Sci.* **1982**, *10*, 143.
(18) Deleted in proof.
(19) Redhead, P. *Vacuum* **1962**, *12*, 203.
(20) Peuckert, M. *J. Phys. Chem*. **1985**, *89*, 2481.
(21) Dunphy, J. C.; McIntyre, B. J.; Gomez, J.; Ogletree, D. F.; Somorjai, G. A.; Salmeron, M. B. *J. Chem. Phys.* **1994**, *100*, 6092.
(22) Schmidt, M.; Wolter, H.; Schick, M.; Kalki, K.; Wandelt, K. *Surf. Sci.* **1993**, *287/288*, 983.
(23) Malik, I. J.; Hrbek, J. J. *Phys. Chem*. **1991**, *95*, 2466.
(24) Engel, T.; Ertl, G. *J. Chem. Phys.* **1978**, *69*, 1267.